The Journal of Chemical Physics

Effect of carbon hybridization in C—F bond as an electron donor in triel bonds

Cite as: J. Chem. Phys. **153**, 074304 (2020); https://doi.org/10.1063/5.0018950
Submitted: 19 June 2020 . Accepted: 29 July 2020 . Published Online: 17 August 2020

Qingqing Yang, Zongqing Chi, Qingzhong Li, and Steve Scheiner

The Journal of Chemical Physics ARTICLE scitation.org/journal/jcp

Effect of carbon hybridization in C—F bond as an electron donor in triel bonds

Cite as: J. Chem. Phys. 153, 074304 (2020); doi: 10.1063/5.0018950
Submitted: 19 June 2020 • Accepted: 29 July 2020 •
Published Online: 17 August 2020

Qingqing Yang,[1] Zongqing Chi,[1] Qingzhong Li,[1,a)] and Steve Scheiner[2,a)]

AFFILIATIONS

[1]The Laboratory of Theoretical and Computational Chemistry, School of Chemistry and Chemical Engineering, Yantai University, Yantai 264005, People's Republic of China
[2]Department of Chemistry and Biochemistry, Utah State University, Logan, Utah 84322-0300, USA

[a)]**Authors to whom correspondence should be addressed:** liqingzhong1990@sina.com and steve.scheiner@usu.edu

ABSTRACT

The ability of the F atom of HC≡CF, H_2C=CHF and H_3CCH_2F to serve as an electron donor to the triel (Tr) atom of TrR_3 in the context of a triel bond is assessed by *ab initio* calculations. The triel bond formed by C_{sp3}—F is strongest, as high as 30 kcal/mol, followed by C_{sp2}—F, and then by C_{sp}—F whose triel bonds can be as small as 1 kcal/mol. The noncovalent bond strength diminishes in the order Tr = Al > Ga > B, consistent with the intensity of the π-hole above the Tr atom in the monomer. The triel bond strength of the Al and Ga complexes increases along with the electronegativity of the R substituent but is largest for R=H when Tr=B. Electrostatics play the largest role in the stronger triel bonds, but dispersion makes an outsized contribution for the weakest such bonds.

INTRODUCTION

Noncovalent interactions play an important role in many fields such as crystalline materials,[1–3] chemical reactions,[4–6] molecular recognition,[7–9] and biological systems.[10–12] Now thousands of studies involving noncovalent interactions are reported each year. One of the goals is to explore which species can serve as electron donors in such interactions, and how effective they might be. The most common electron donors are the lone pairs of atoms, either on halogen atoms or on oxygen, nitrogen, etc. The electron donor capability of halogens has attracted a good deal of attention.[13–17] These halogen species include carbon-bound and terminal metal-bound halogens and halide ions. Anion recognition, particularly for F^- and Cl^-, has been realized by means of hydrogen bond (HB) and/or halogen bond (XB),[7,8] utilizing the anion as a particularly effective electron donor. Halide ions form a stronger noncovalent interaction with smaller anions: $F^- > Cl^- > Br^- > I^-$. Halide ligands (M-X) have also been demonstrated to be excellent electron donors in HBs and XBs. Interest in noncovalent interactions involving halide ligands centers around molecular building blocks, constructing functional materials with magnetic, thermochromic, and photoelectric properties.[18] Organic halogens bonded to carbon are also a focus since halocarbons are extensively present in organic molecules. It is usually accepted that halocarbons are much poorer electron donors in HBs than halide ions and halide ligands.

Due to its electron-deficient nature, boron trihydride (BH_3) and boron trihalides (BX_3) are often used to bind with small molecules such as HCN and NH_3, forming a partially covalent Lewis acid–base complex suggested by Leopold and co-workers.[19–21] Such complexes have attracted interest since they have been postulated early on as transition states in S_N2 reactions such as the reactions of borine carbonyl (BH_3—CO) and trimethylamine[22,23] as well as the borate–fluorine bond cleavage reaction by electron-rich late-transition metal complexes.[24] In such a S_N2 reaction, a pentacoordinate boron compound is formed, and this type of compound has been isolated.[25] According to the molecular electrostatic potential (MEP) analysis, the boron atom in the tricoordinate boron compound has a positive MEP region, often termed a π-hole, which lies above the molecular plane.[26] Besides boron, other atoms in the same group also participate in a similar interaction, frequently called a triel bond (TrB), which occurs between the π-hole on the triel atom and an electron donor.[27]

The TrB displays some unexpected properties. The π-hole on the BF_3 molecule is larger than that on the BH_3 molecule, but yet a stronger triel bond is found for the latter molecule.[28] TrB can combine with HB, XB, or pnicogen bond (ZB),[20,29,30] displaying cooperativity. In $BF_3\cdots NCH\cdots NCH$, $BF_3\cdots NCX\cdots NCH$ (X = halogen), and $BF_3\cdots NCZH_2\cdots NH_3$ (Z = P, As, Sb), the TrB shows a positive cooperativity with the HB, XB, or ZB, and both interactions enhance one another.[20,29,30] However, the intermolecular distance in the stronger TrB is shortened by more than the other interaction,[20,29,30] opposite to the usual conclusion that the larger contraction takes place for the weaker interaction.[31] These unexpected variations are to a great extent ascribed to prominent distortion of the tricoordinate triel molecule in the formation of a TrB, which is changed from a planar structure in the isolated molecule into a pyramidal geometry in the complex.[32] This larger deformation stresses the importance of polarization for the formation of a TrB.[33] Even so, the TrB is steered by the same mechanism as HB and XB in which charge transfers from the Lewis base to the Lewis acid unit.[34]

There has been some research in the past that probed the possibility of various TrB electron donors, not only conventional lone pairs, anions,[35] but also π-electron systems[36–38] and even more unconventional electron donors such as metal hydrides,[39,40] radicals,[41] and carbenes.[42] A TrB can be very strong, with interaction energies reaching more than 100 kcal/mol. On the other end of the spectrum, the dihydrogen bond between phenol and diethylmethylsilane is very weak (3 kcal/mol),[43] indicating that the Si—H bond is a weak electron donor. Nonetheless, this weak donor can still manage to form a strong TrB with BH_3 (40 kcal/mol).[39] In the study of TrBs, the usual electron donors are oxygen-containing and nitrogen-containing molecules.[44] Very recently, for example, our group[45] compared the TrB with different chalcogen electron donors, and it was found that the TrB is stronger in the O > S ≈ Se order.

Besides these common donors, TrBs with halogens as the donor have been subject to some examination. The complexes of $BH(CO)_2/BH(N_2)_2$ with XF_3/XF_5 (X = Cl, Br, and I) are bonded by a combination of a XB and a TrB, where the XB makes a larger contribution than the TrB.[46] This TrB is formed between the σ-hole on the B atom along the B—H bond, and the negatively charged F atom. BH_2X (X = F, Cl, Br, and I) can form a dimer through hydrogen, halogen, or triel bonding interactions, of which the most stable dimer is primarily stabilized by triel bonding. Interestingly, the B···X triel-bond is stronger for the heavier halogen atom, opposite to the negative electrostatic potential on the X atom.[47] In the triel-bonded complexes using a halogen anion as the electron donor, the interaction becomes stronger for the lighter halogen anion.[35] Moreover, the triel-boned complexes using two triel atoms bonded to an anion are so very stable that they can be found in some crystal structures.[44]

However, none of the above studies of TrBs considered carbon-bound halogens, so the concept of a halogen atom acting as an electron donor in a triel bond represents untrodden ground. However, such a role for organic F is widely known, not only in the context of crystal engineering but also in the design of functional materials.[48] Although Dunitz and Taylor concluded that organic fluorine is not a good electron donor in HBs,[49] the triel bond is quite different in some respects so it is important to assess F in this context. The research described below represents a first attempt to rectify this deficiency. As a Lewis acid, a set of TrR_3 molecules are considered. As a central Tr atom, B, Al, and Ga are considered so as to examine the dependence on the size of the triel atom. Substituents R include H, F, Cl, and Br, which thus offer a wide range of electron-withdrawing capacity. The electron donating F atom is attached to a C atom, which takes on one of three hybridizations. This C is sp^3-hybridized in CH_3CH_2F but takes on sp^2-hybridization in $CH_2{=}CHF$, while CH_3CH_2F presents sp-hybridization. All combinations of these systems are considered, making for a total of 36 different heterodimers. The research seeks to first determine whether or not a C—F bond can participate in a triel bond. The work then proceeds to assess the effects of the size of the triel atom, the electronegativity of the three substituents, and the hybridization of the C atom to which the F atom is bound. The calculations finally address the fundamental aspects of these triel bonds, what are their most basic physical origins.

THEORETICAL METHODS

Gaussian09 software was utilized to perform all calculations of complexes and monomers.[50] All structures were optimized at the MP2/aug-cc-pVTZ level. To insure a minimum, frequency calculations were then carried out for these species at the same level. The interaction energy E^{int} compared the energy of the complex with the sum of monomers within the geometry adopted within the dimer. The binding energy E_b takes as its reference the monomers in their fully optimized structures. Deformation energy is defined as the difference between the two, the energy required for the pair of monomers to adjust their geometry for complexation. The Boys and Bernardi counterpoise method[51] was used to correct the basis set superposition error (BSSE) for both E^{int} and E^b.

The molecular electrostatic potentials (MEPs) of the monomers on the 0.001 a.u. isodensity surface were evaluated at the MP2/aug-cc-pVTZ level by means of the Wave Function Analysis-Surface Analysis Suite program.[52] AIM2000 software[53] was applied to obtain the electron density, Laplacian, and energy density at the relevant bond critical points (BCPs). Using the NBO3.0 package[54] in the Gaussian09 software, the natural bond orbital analysis was performed at the HF/aug-cc-pVTZ level to obtain orbital interaction and charge transfer data. By means of the LMOEDA (localized molecular orbital energy decomposition analysis) method[55] in the GAMESS program,[56] the total interaction energy was decomposed at the MP2/aug-cc-pVTZ level, and five kinds of energy with physical significance were obtained: electrostatic energy (E^{ele}), exchange energy (E^{ex}), repulsion energy (E^{rep}), polarization energy (E^{pol}), and dispersion energy (E^{disp}).

RESULTS

sp alkynes

All of the complexes of HC≡CF with TrR_3 take on a geometry like that pictured in Fig. 1. The F atom of HCCF lies close to the C_3 axis of TrR_3 at a distance R from the Tr atom. The HCCF molecule is turned by an angle α so that one of the F lone pairs can

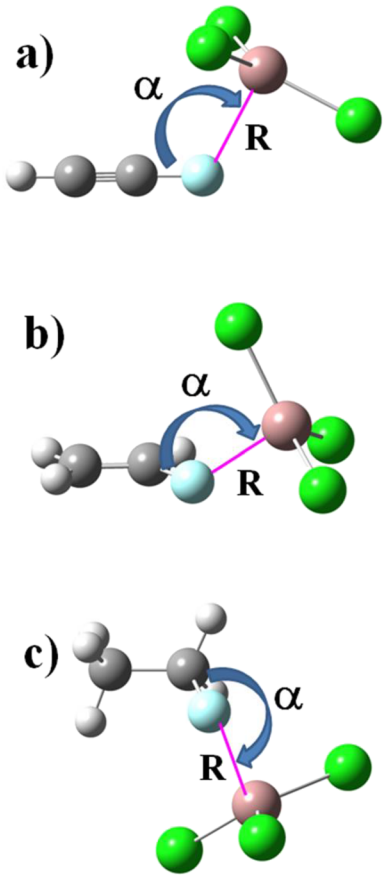

FIG. 1. Geometries of the complexes of (a) HCCF, (b) $H_2C{=}CHF$, and (c) $H_3C{-}CH_2F$ with TrR_3.

optimally approach the Tr atom. Note that this orientation is also consistent with the minima on the HCCF MEP. The distance R and angle α of the various complexes are all listed in Table I along with energetic properties. The α angle varies between 102° and 124°, typically largest for TrF_3 in any subset of a particular Tr atom. This may be due, in part, to Coulombic repulsions between the F atoms on the TrF_3 and the negative regions on the HCCF unit. It is also the TrF_3 molecule that has the shortest intermolecular R distance, with the exception of Tr=B, where it is shorter for TrH_3. With regard to energetics, the interaction energies range between −0.9 kcal/mol and −5.5 kcal/mol. These quantities increase in the order B < Ga < Al and for any given Tr atom R = H < Br < Cl < F, i.e., increasing electronegativity.

Table II displays a quantitative assessment of the charge shifts in the complexes. CT refers to the total amount of density shifted between molecules from HCCF to TrR_3, while $E^{(2)}$ focuses on one particular inter-orbital transfer, from a lone pair of F to the unfilled lone pair orbital of Tr, essentially a *p*-orbital. These measures of charge transfer mirror the energetics reasonably well: they are also largest for Al and smallest for B and rise along with the electronegativity of R (with the exception of Tr=B for which H is largest). Other

TABLE I. Interaction energy E^{int}, binding energy E^b, deformation energy DE, all in kcal/mol, Tr···F intermolecular distance (R), and C—F···Tr angle (α) in the complexes.

Complexes	$E^{int,a}$	E^b	DE	R (Å)	α (deg)
C_{sp}—F					
BH_3	−1.11	−1.09	0.02	2.556	113.5
BF_3	−0.94	−0.92	0.02	2.711	115.5
BCl_3	−1.66	−1.66	0.00	2.984	103.3
BBr_3	−1.79(−1.89)	−1.79	0.00	2.982	102.2
AlH_3	−2.21	−1.98	0.23	2.469	119.2
AlF_3	−5.51	−4.17	1.34	2.160	121.9
$AlCl_3$	−3.96	−3.02	0.94	2.310	120.3
$AlBr_3$	−3.24(−3.35)	−2.57	0.67	2.393	118.7
GaH_3	−1.23(−1.28)	−1.07	0.16	2.461	120.8
GaF_3	−3.16(−3.26)	−2.19	0.97	2.189	123.7
$GaCl_3$	−2.31(−2.34)	−1.83	0.48	2.403	120.3
$GaBr_3$	−2.11(−2.20)	−1.85	0.26	2.527	116.9
C_{sp2}—F					
BH_{3+}	−4.22	−3.32	0.90	2.130	114.3
BF_3	−3.31	−2.98	0.33	2.468	118.1
BCl_3	−2.78	−2.70	0.08	2.799	109.5
BBr_3	−2.47(−2.56)	−2.41	0.06	2.826	107.1
AlH_3	−11.09	−8.79	2.30	2.113	120.5
AlF_3	−21.32	−15.61	5.71	1.960	123.1
$AlCl_3$	−19.08	−13.27	5.81	1.983	121.8
$AlBr_3$	−17.35(−17.52)	−11.84	5.51	1.992	122.0
GaH_3	−6.24(−6.12)	−4.90	1.34	2.204	121.7
GaF_3	−15.83(−15.87)	−11.64	4.19	2.034	123.7
$GaCl_3$	−11.47(−11.36)	−8.07	3.40	2.104	121.3
$GaBr_3$	−9.84(−9.93)	−6.71	3.13	2.133	120.1
C_{sp3}—F					
BH_3	−9.95	−6.10	3.85	1.856	114.8
BF_3	−5.69	−4.67	1.02	2.283	115.4
BCl_3	−3.73	−3.51	0.22	2.662	113.0
BBr_3	−3.35(−3.45)	−3.15	0.20	2.693	110.9
AlH_3	−17.15	−13.81	3.34	2.026	117.9
AlF_3	−29.74	−22.42	7.32	1.910	121.7
$AlCl_3$	−27.45	−20.12	7.33	1.918	121.8
$AlBr_3$	−26.00(−26.18)	−18.82	7.18	1.922	121.6
GaH_3	−10.15(−9.98)	−8.16	1.99	2.130	116.8
GaF_3	−23.05(−23.13)	−17.60	5.45	1.987	120.4
$GaCl_3$	−18.24(−18.09)	−13.48	4.76	2.034	120.3
$GaBr_3$	−16.33(−16.41)	−11.79	4.54	2.052	119.9

[a]Data in parentheses refer to interaction energies calculated at the MP2/aug-cc-pVTZ(PP) level.

gauges of bond strength arise from AIM analysis of the electron density topology, data for which are listed in Table III. The density (ρ), its Laplacian ($\nabla^2\rho$), and the energy density (H) all refer to the bond critical point between F and Tr. Like the charge transfer parameters in Table II, the atoms in molecules (AIM) measures of noncovalent bond strength conform to the same general patterns as do the energetics, with the exception that the Ga quantities exceed the Al values.

TABLE II. Charge transfer (Q, *e*) from F-containing molecule to TrR_3 and NBO perturbation energy [$E^{(2)}$, kcal/mol] for transfer from the F lone pair to the Tr unfilled lone pair orbital.

	C_{sp}—F		C_{sp2}—F		C_{sp3}—F	
Complexes	Q	$E^{(2)}$	Q	$E^{(2)}$	Q	$E^{(2)}$
BH_3	0.0140	8.23	0.0537	38.09	0.1177	...
BF_3	0.0040	1.56	0.0106	6.36	0.0230	15.17
BCl_3	0.0044	2.84	0.0091	6.16	0.0143	11.09
BBr_3	0.0058	4.28	0.0104	8.96	0.0160	13.83
AlH_3	0.0300	19.93	0.0722	57.52	0.0892	71.51
AlF_3	0.0435	32.19	0.0778	67.08	0.0918	80.33
$AlCl_3$	0.0421	33.83	0.0909	80.10	0.1050	...
$AlBr_3$	0.0384	31.77	0.0894	78.39	0.1029	89.05
GaH_3	0.0294	20.98	0.0618	48.35	0.0779	60.93
GaF_3	0.0431	29.59	0.0729	55.25	0.0880	67.68
$GaCl_3$	0.0358	27.48	0.0793	65.64	0.0948	77.85
$GaBr_3$	0.0292	23.52	0.0747	63.71	0.0911	76.14

TABLE III. Electron density (ρ), its Laplacian ($\nabla^2\rho$), and energy density (H) at the intermolecular F···Tr BCP, all in a.u.

Complexes	ρ	$\nabla^2\rho$	H
C_{sp}—F			
BH_3	0.0091	0.0424	0.0015
BF_3	0.0064	0.0319	0.0016
BCl_3	0.0053	0.0224	0.0010
BBr_3	0.0057	0.0232	0.0010
AlH_3	0.0106	0.0470	0.0011
AlF_3	0.0194	0.1582	0.0078
$AlCl_3$	0.0148	0.0853	0.0029
$AlBr_3$	0.0131	0.0614	0.0014
GaH_3	0.0169	0.0947	0.0032
GaF_3	0.0332	0.2139	0.0034
$GaCl_3$	0.0200	0.1092	0.0031
$GaBr_3$	0.0155	0.0757	0.0024
C_{sp2}—F			
BH_3	0.0226	0.0886	−0.0001
BF_3	0.0116	0.0520	0.0019
BCl_3	0.0076	0.0304	0.0012
BBr_3	0.0078	0.0305	0.0011
AlH_3	0.0249	0.1883	0.0077
AlF_3	0.0378	0.3468	0.0142
$AlCl_3$	0.0367	0.3126	0.0119
$AlBr_3$	0.0362	0.3051	0.0115
GaH_3	0.0337	0.2083	0.0028
GaF_3	0.0540	0.3622	−0.0001
$GaCl_3$	0.0453	0.2820	0.0006
$GaBr_3$	0.0423	0.2577	0.0010
C_{sp3}—F			
BH_3	0.0401	0.1136	−0.0120
BF_3	0.0172	0.0682	0.0008
BCl_3	0.0098	0.0392	0.0014
BBr_3	0.0099	0.0378	0.0013
AlH_3	0.0324	0.2670	0.0106
AlF_3	0.0455	0.4209	0.0150
$AlCl_3$	0.0453	0.3993	0.0136
$AlBr_3$	0.0452	0.4015	0.0135
GaH_3	0.0420	0.2651	0.0014
GaF_3	0.0631	0.4239	−0.0034
$GaCl_3$	0.0559	0.3574	−0.0018
$GaBr_3$	0.0535	0.3384	−0.0010

The division of the total interaction energy into its constituent parts is displayed in Table IV. The attractive part of the exchange energy is the largest component, with the other terms somewhat lower. The dispersion energy exceeds the other two for BR_3, but the reverse is true for the other two Tr atoms. E^{ele} and E^{pol} are generally comparable to one another although the former tends to be larger than the latter.

One can consider the disposition of the molecular electrostatic potential (MEP) surrounding each monomer as a means of helping understand the geometry adopted by a given dimer. The MEP of HC≡CF in Fig. 2(a) does not have an extreme negative region near the F atom, which would have been blue in this diagram. The most negative region is a ring around the F atom, with a $V_{s,min}$ of only −0.0064 a.u. Its position off of the HCCF axis helps to explain the deviation of the α angle from 180°. The small value of $V_{s,min}$ is consistent with the relatively small electrostatic energy, especially when compared to the other complexes below.

Each TrR_3 molecule contains a positive region, or π-hole, directly above and below the Tr atom. The value of the maximum is reported in Table V and shows some clear trends. For any particular substituent R, the π-hole above Al is the most intense, followed by Ga and then B. This order comports with the Tr electronegativity (B: 2.0, Al: 1.6, Ga: 1.8). $V_{s,max}$ is consistently largest for R=F, followed by Cl and then Br with the latter two being much smaller than F. The placement of H in this hierarchy is somewhat variable and depends upon Tr. This pattern is not entirely consistent with the electrostatic energies in Table IV. For example, TrF_3 does not have the largest E^{ele} for B and Al.

sp^2 alkenes

When combined with H_2C=CHF, the TBr_3 unit situates itself above the alkene's molecular plane, as indicated by a typical such structure in Fig. 1(b). The R(Tr···F) distances and α angles are displayed in the second section of Table I where it may be seen that the intermolecular distances are much shorter than for the HCCF sp-hybridized structures in the first section. These contractions vary from 0.15 Å to as much as 0.43 Å, while the α(C—F···Tr) angles change by only a few degrees. Along with the closer contact in the sp^2 cases, there is a very substantial rise in the interaction energies. The smallest such increments of 0.7 kcal/mol–3.1 kcal/mol arise in the BR_3 complexes, but even here, the percentage increases are impressive, from 38% to 280%. The interaction energies for Al and Ga also increase substantially, by a factor

TABLE IV. Electrostatic (E^{ele}), exchange (E^{ex}), repulsion (E^{rep}), polarization (E^{pol}), and dispersion (E^{disp}) energies in $TrR_3\cdots H_2X$. All in kcal/mol.

Complexes	E^{ele}	E^{ex}	E^{rep}	E^{pol}	E^{disp}
C_{sp}—F					
BH_3	−1.33	−4.20	7.34	−0.75	−2.19
BF_3	−0.88	−2.30	4.16	−0.56	−1.39
BCl_3	−1.02	−4.80	8.12	−0.37	−3.63
BBr_3	−1.59	−7.13	12.05	−0.50	−4.64
AlH_3	−3.71	−8.43	15.61	−3.16	−2.65
AlF_3	−6.50	−11.01	22.39	−9.56	−1.23
$AlCl_3$	−7.25	−16.51	31.29	−7.23	−4.49
$AlBr_3$	−7.10	−17.43	32.41	−6.03	−5.25
GaH_3	−4.00	−9.56	17.88	−2.76	−2.82
GaF_3	−7.64	−13.67	28.01	−9.04	−0.85
$GaCl_3$	−6.20	−14.79	28.00	−5.18	−4.18
$GaBr_3$	−5.30	−14.16	26.02	−3.76	−4.93
C_{sp2}—F					
BH_3	−9.66	−18.55	33.79	−5.36	−4.47
BF_3	−5.69	−6.46	11.92	−1.75	−1.35
BCl_3	−3.48	−8.23	14.00	−0.97	−4.12
BBr_3	−3.87	−10.20	17.52	−1.23	−4.70
AlH_3	−20.93	−25.71	49.58	−11.68	−2.59
AlF_3	−29.66	−23.14	48.64	−19.29	1.47
$AlCl_3$	−32.03	−38.52	75.92	−22.05	−2.87
$AlBr_3$	−33.82	−44.06	86.41	−22.76	−3.48
GaH_3	−17.82	−24.76	47.44	−8.15	−2.94
GaF_3	−30.27	−27.60	57.46	−17.12	1.70
$GaCl_3$	−27.10	−35.34	69.65	−15.63	−3.02
$GaBr_3$	−26.93	−38.99	75.62	−15.29	−4.18
C_{sp3}—F					
BH_3	−23.89	−42.50	79.87	−16.53	−6.98
BF_3	−10.81	−12.33	23.03	−3.81	−1.82
BCl_3	−5.77	−11.42	19.65	−1.78	−4.43
BBr_3	−6.38	−15.12	25.84	−2.11	−5.58
AlH_3	−30.61	−34.02	65.84	−16.06	−2.62
AlF_3	−40.73	−28.17	59.69	−23.25	1.91
$AlCl_3$	−44.51	−46.03	91.64	−27.17	−1.97
$AlBr_3$	−47.03	−54.39	106.81	−28.94	−2.92
GaH_3	−25.76	−33.19	63.67	−11.30	−3.55
GaF_3	−41.16	−33.92	71.08	−20.85	1.80
$GaCl_3$	−38.94	−45.16	89.28	−20.56	−2.81
$GaBr_3$	−39.26	−50.77	98.71	−20.87	−4.03

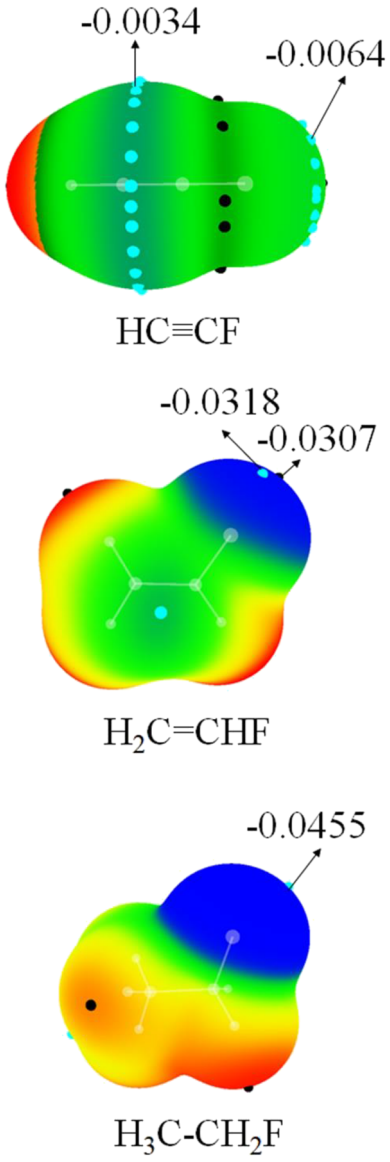

FIG. 2. MEP maps of HC≡CF, H_2C=CHF, and H_3C—CH_2F on the ρ = 0.001 a.u. isodensity surface. Color ranges, in a.u., are: red, greater than 0.02; yellow, between 0.02 and 0; green, between 0 and −0.02; and blue, smaller than −0.02. Small blue and black spheres indicate the position of maxima and minima, respectively.

of 3–4. The trends are consistent: for both Al and Ga, the binding energies diminish in order R = F > Cl > Br > H, and AlR_3 engages in stronger complexes than does GaR_3. The BR_3 complexes are most weakly bound of all with R=H forming the strongest bond.

Along with the better energetics of the sp^2 complexes are larger measures of charge transfer. As exhibited in Table II, the total intermolecular transfer Q varies from a low of 0.01*e* to as much as 0.09*e*. These quantities represent a 70%–280% enhancement relative to the sp dimers. The magnifications are quite similar for the $E^{(2)}$ measure of inter-orbital transfer, which increases by 90%–360%. The largest charge transfer parameters do not necessarily coincide with the strongest bond; for example, the R=Cl and Br quantities exceed those for R=F. AIM measures of triel bond strength also are amplified by the conversion from sp to sp^2. The bond critical point density, for example, grows by 40%–180%; the growth of the Laplacian is even larger, as much as 400%. The trends in these AIM parameters more closely adhere to energetics, being largest for R=F (again with the exception of Tr=B).

TABLE V. Values of $V_{s,max}$ (au) for TrR_3 monomers, along the C_3 axis of each molecule.

	TrH_3	TrF_3	$TrCl_3$	$TrBr_3$
B	0.0753	0.1123	0.0578	0.0489
Al	0.1395	0.2626	0.1462	0.1245
Ga	0.1150	0.2065	0.1315	0.1125

The various components of the interaction energies are generally magnified by the sp → sp^2 transition. The electrostatic element, for example, is raised by between 140% and 630%, making it clearly the largest contributor after exchange. A somewhat smaller rise in polarization energy places this component second to E^{ele}. The dispersion energy is affected to a much smaller degree, even becoming smaller in certain instances, such that it makes minimal contributions to these complexes.

A glance at Fig. 2(b) reveals an extensive blue region around the F atom of H_2C=CHF, with a MEP minimum of −0.032 a.u. near the extension of the C—F bond. This much more intense minimum correlates with the much larger electrostatic component in Table IV for the sp^2 dimers. However, its placement along the bond axis does not explain the large deviations of α from 180° in Table I. This displacement can be best understood by the presence of secondary interactions in these complexes. In addition to the primary Tr···F triel bond, the H the = CHF group is in position to form a CH···R H-bond to a halogen atom of TrR_3. This H-bond is facilitated by the proximate position of the F, which pulls electron density and more strongly polarizes the C—H bond. These secondary interactions, along with their attendant distances, are displayed in Fig. S1. A more complete listing of secondary interactions as identified by AIM is supplied in Table SI. The bond critical point densities are generally considerably smaller than the triel bond quantities but cannot be ignored. Taking GaF_3 as an example, ρ_{BCP} for the triel bond is 0.0540 a.u., while the same quantity for the secondary bond is 0.0116 a.u. In any case, it is clear that the interaction energies in Table I cannot be attributed exclusively to the triel bond as there are supplements arising from the secondary interactions as well.

sp^3 alkanes

Like the other systems, the complexes containing the sp^3-hybridized H_3CCH_2F also place the Tr atom significantly off the C—F axis, with α angles in the last section of Table I that are within a few degrees of the sp^2 quantities. The intermolecular R(Tr···F) distances, on the other hand, are very considerably shortened by the change to sp^3 hybridization, shrinking by between 0.05 Å and 0.27 Å. As one might expect, this bond contraction is accompanied by a very significant strengthening of the triel bond. The interaction energies grow larger by up to 8.7 kcal/mol. This increase when compared to sp^2 represents a rise by 35%–63% in most cases, with the exception of the more than doubling for BH_3. The trends for the sp^3 series essentially mimic those for the others: R = F > Cl > Br > H for Tr=Al and Ga, but when Tr=B, it is BH_3 that is most strongly bound. Again one sees the trend that Al engages in the strongest triel bonds, followed by Ga and then B.

Like the energetics, the total charge transfer Q on Table II is also magnified for the sp^3 series when compared to sp^2, increasing by 15%–26% for Al and Ga, with larger percentage increases for Tr=B. The $E^{(2)}$ quantities are also enhanced to the point that NBO views the triel bond in the complexes of H_3CCH_2F with both BH_3 and $AlCl_3$ as covalent, so there is no $E^{(2)}$ evaluated. The strength of this bond is further verified by the large AIM parameters in Table III for the sp^3 complexes. Some of the bond critical point densities exceed 0.05 a.u., bordering on a covalent bond. This sort of designation is supported by the negative values of H for the strongest bonds, albeit even if only slightly negative.

The various components of the interaction energy in Table IV, with the exception of dispersion which is relatively static, all undergo an amplification upon sp^3 hybridization of the C—F bond. The electrostatic contribution, for example, rises by roughly 40% and by more than this for Tr=B. This increase is consistent with the larger value of $V_{s,min}$ on $H_3C—CH_2F$, which is −0.046 a.u., as compared to −0.032 a.u. for H_2C=CHF. The polarization energy also rises by some 20%–30% in most cases but again higher for Tr=B.

Like the previous case of H_2C=CHF, $H_3C–CH_2F$ also engages in secondary attractive interactions, mostly CH···X H-bonds. The most prominent of these are displayed in Fig. S2, which are largely responsible for the nonlinear α(CF···Tr) angles. The last section of Table SI in the supplementary material reports the AIM quantities of those secondary interactions that result in a bond path. As in the sp^2 cases, the triel bond parameters clearly exceed those of the secondary quantities, but note also that there can be more than one such secondary bond. GaF_3, for example, has a triel bond critical point density with H_3CCH_2F of 0.0631 a.u., which is complemented by three secondary bonds with densities of 0.0090 a.u., 0.0057 a.u., and 0.0051 a.u., respectively. So again, the interaction energies of many of the sp^3 systems cannot be considered as the exclusive province of the triel bond.

DISCUSSION

As was noted above for each C-hybridization separately, the electrostatic and polarization energies roughly mirror the behavior of the total interaction energy. In fact, this approximation spans all three hybridizations. Figure 3(a) displays a rough linear relationship between E^{int} and E^{ele} for all systems combined, with the correlation coefficient R^2 = 0.92. The correlation is slightly poorer for E^{pol}, with R^2 = 0.90, as indicated in Fig. 3(b). The slope of 1.68 in Fig. 3(a) shows that the electrostatic energy rises more quickly than does the total interaction energy, while the slope is much closer to unity for the polarization energy in Fig. 3(b).

The engagement with the electron-donating molecule causes each TrR_3 molecule to distort from its planar geometry into a trigonal pyramid shape. The energetic consequence of this deformation is encapsulated in the deformation energy (DE) quantities in Table I. DE correlates very roughly with the strength of the triel bond. For example, the HC≡CF interaction energies do not exceed 5 kcal/mol, and DE similarly peaks at 1 kcal/mol. However, the interactions with H_2C=CHF which can exceed 20 kcal/mol correspond to deformation energies of almost 6 kcal/mol. As the interaction energies rise further with $H_3C—CH_2F$, up to 30 kcal/mol, the DE climbs above 7 kcal/mol. Furthermore, there is a clear correlation between

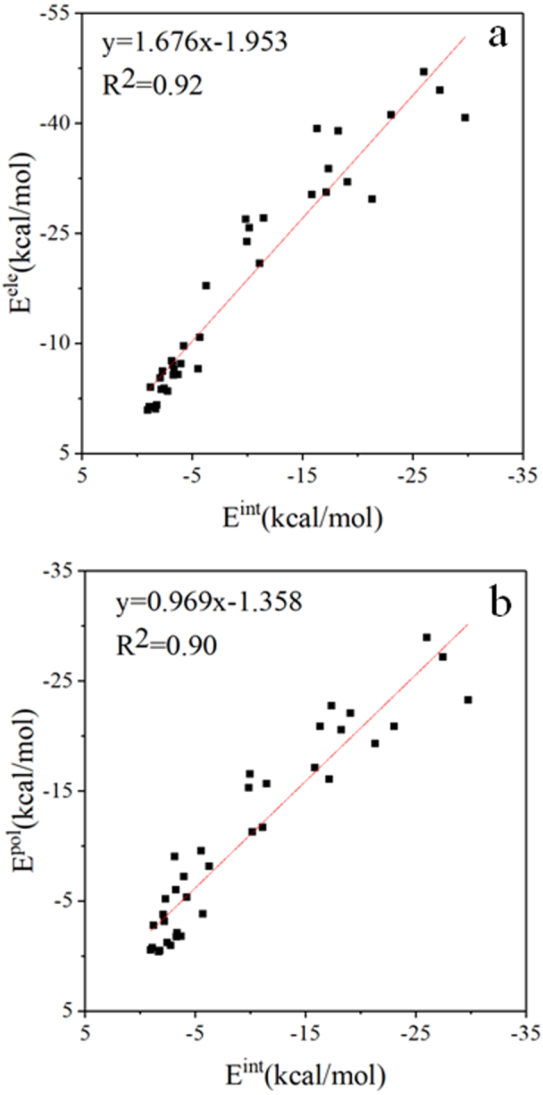

FIG. 3. Relationship between the interaction energy and (a) the electrostatic and (b) polarization energies.

the geometric distortion of TrR_3 and the dissociation energy. Figure S3 documents a quadratic relationship between the mean angle of R—Tr···F (β) and DE where $\beta = 91 + 2.3DE + 0.16(DE)^2$, a relationship which bears a correlation coefficient $R^2 = 0.97$.

The total amount of charge density transferred from the electron donor to the acceptor reaches its maximum of 0.118*e* in $H_3C—CH_2F···BH_3$, although CT is less than 0.1e for most of the complexes here. This quantity is much smaller than the charge transfer in triel bonds formed by carbene, O/N electron donors (generally greater than 0.2*e*, even close to 0.8*e*).[42]

For both sp^2 and sp^3 hybridizations, QTAIM parameters suggest that GaF_3 species participate in partly covalent interactions while AlF_3 does not, even though the latter is the stronger Lewis acid. The Wiberg bond index (WBI) between the Tr and F atoms listed in Table S2 is larger in the AlF_3 complexes than for GaF_3, indicating that the Al···F triel bond has a stronger covalent component than does Ga···F. The energy density is sometimes a highly negative value for an ionic bond.[57] One should thus be cautious in characterizing the covalent nature of a triel bond purely by means of QTAIM parameters.

There are some different trends for the B complexes and their Al/Ga counterparts in Fig. 4. The Al···F and Ga···F triel-bonded complexes become more stable with the increase in R electronegativity. This is also true for the B···F triel-bonded complexes in both sp^2 and sp^3 hybridizations except that R = H has the largest interaction energy. For sp hybridization, however, the B···F triel-bonded complexes have increasing interaction energy in the order R = F < H < Cl < Br, different than that in both sp^2 and sp^3 hybridizations. These trends are not completely consistent with the positive MEP on the π-hole of the triel atom. Both E^{int} and E^b are consistent with one another, so the inconsistency cannot be attributed to distortion of TrR_3. Some inconsistent variations are also found between E^{int} and the Wiberg bond index of Tr···F triel bond. Therefore, the different trends in Fig. 4 are possibly due to the secondary interactions even including repulsion interaction.

With regard to any possible relativistic effects arising for the larger atoms, interaction energies for systems containing Br and Ga were recalculated at the MP2/aug-cc-pVTZ(PP) level, which includes some account of relativistic effects. Their strong similarity with the aug-cc-pVTZ data indicates only very minimal relativistic effects.

The F atom has been considered as the nucleophilic source of electron density in triel bonds in the past, but the pertinent F was not bonded to C in an organic system. Nonetheless, these past studies can provide illuminating context for the results presented here. As one example, the BH_2X (X = F, Cl, and Br) dimer is held together by

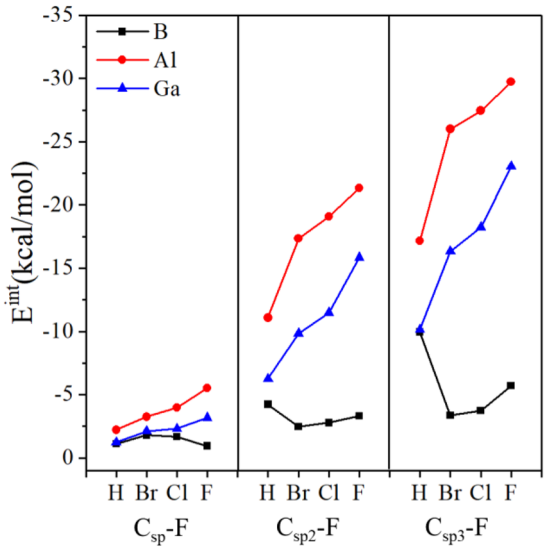

FIG. 4. Relationship between total interaction energies and nature of Tr and R atoms in TrR_3.

a pair of triel bonds with BX as an electron donor.[47] The interaction energy of the BH_2F homodimer is −8.8 kcal/mol at the RI-MP2/aug-cc-pVQZ level, so each triel bond contributes −4.4 kcal/mol,[47] making the B—F bond a better electron donor than the C_{sp}—F bond, perhaps somewhere between the C_{sp2}—F and C_{sp3}—F bonds. Complexes between $BH(CO)_2/BH(N_2)_2$ and XF_3/XF_5 (X = Cl, Br, and I) are stabilized by both a halogen bond and a triel bond with B···F separation of 2.1 Å–2.9 Å,[46] not unlike the 1.8 Å–3.0 Å range of the BR_3···F—C systems considered here. Of course, replacing a neutral R—F bond of any sort by a fluoride anion would raise the interaction energy.[35]

As mentioned earlier, the F atom is not the most commonly studied electron donor in triel bonds, so it is of interest to compare it to others, e.g., N and O. The B···O triel bond strength in R_3B···OH_2 has little correlation with the particular substituent R, while the Al/Ga···O triel bond strength is clearly correlated with the R electronegativity,[45] much like the trends in Table I. The weak *N*-electron donor N_2 forms a B···N triel bond with interaction energy less than −2 kcal/mol,[58] similar to that seen here for the C_{sp}—F electron donor. In an interesting reversal, the triel bond involving NCH grows stronger in the order $BF_3 < BCl_3 < BBr_3$,[58] opposite to that for the C_{sp2}—F and C_{sp3}—F complexes described above. For an even stronger nucleophile such as NH_3, the bond strength sequence becomes $BF_3 < BCl_3 \approx BBr_3$.[58] It appears then that the dependence of triel bond strength on the B-substituent is a complicated one.

With regard to triel-bonding center, with N_2 and HCN bases,[59] the bond becomes stronger from BR_3 to GaR_3 to AlR_3, consistent with the C—F electron donor pattern seen here. For NH_3, on the other hand, BCl_3 forms a stronger triel bond than does $AlCl_3$.[59] The latter pattern persists for *N*-heterocyclic carbene as an electron donor.[42] This unusual result can be partly attributed to the facile distortion of BR_3 caused by a strong electron donor.

Extending the scope beyond triel bonds, previous studies have shown that C—F can serve as an electron donor in both HBs[60] and XBs.[61] However, these bonds are typically quite weak. For example, the HB interaction energy involving the C—F electron donor seldom exceeds −4 kcal/mol.[62] However, for the triel bond, the interaction energy is often larger than −4 kcal/mol when the C_{sp2}—F and C_{sp3}—F act as an electron donor. That is, the C—F bond appears to be a better electron donor in triel bonds than is the case in either HBs or XBs.

CONCLUSIONS

Organic fluorine connected with differently hybridized C atoms can serve in the capacity of an electron donor to form a triel bond with TrR_3, and its strength is related to the hybridization of C, as well as the nature of both Tr and R. These relationships are most plainly visible in Fig. 4. For any C hybridization, the Al complexes are more strongly bound than Ga, which are, in turn, stronger than B. For both Al and Ga, the bond grows stronger in the order R = H < Br < Cl < F, i.e., with greater electronegativity. The same is true for Tr = B except that R = H forms a stronger bond than the others for both sp^2 and sp^3 hybridizations. Perhaps the most obvious trend in Fig. 4 is the progressive strengthening of the triel bond as one advances from sp to sp^2 to sp^3. Altogether, the triel bonds span a wide range of interaction energy, from only 1 kcal/mol for Tr = B to as much as 30 kcal/mol for $H_2C{=}CHF{\cdots}AlF_3$.

NBO analysis shows that the principal orbital interaction of these triel bonds involves transfer from the lone pair of a Lewis base F to the empty p orbital of the Tr atom, regardless of the C hybridization. AIM confirms this triel bond as well as certain supplementary weaker C—H···X H-bond and F···C interactions. The relative magnitudes of electrostatic, polarization, and dispersion energies are generally similar. Most of the complexes are dominated by electrostatics, but in some weak complexes, especially those involving B, the dispersion contribution is prominent.

The F—Tr dative bond has been found in several crystal structures,[63,64] but no theoretical study has heretofore treated the C—F···Tr triel bond. This study will hopefully lead to a greater understanding of this type of triel bond with C—F as electron donor.

SUPPLEMENTARY MATERIAL

See the supplementary material for Figs. S1–S3, Tables S1 and S2, and Cartesian coordinates.

ACKNOWLEDGMENTS

This work was supported by the National Natural Science Foundation of China (Grant No. 21573188).

DATA AVAILABILITY

The data that support the findings of this study are available within the article and its supplementary material.

REFERENCES

[1] A. Saha, S. A. Rather, D. Sharada, and B. K. Saha, Cryst. Growth Des. **18**, 6084–6090 (2018).
[2] F. Zordan and L. Brammer, Cryst. Growth Des. **6**, 1374–1379 (2006).
[3] D. E. Arkhipov, A. V. Lyubeshkin, A. D. Volodin, and A. A. Korlyukov, Crystals **9**, 242 (2019).
[4] S. M. Walter, F. Kniep, E. Herdtweck, and S. M. Huber, Angew. Chem., Int. Ed. **50**, 7187–7191 (2011).
[5] P. La Manna, M. De Rosa, C. Talotta, A. Rescifina, G. Floresta, A. Soriente, C. Gaeta, and P. Neri, Angew. Chem. **132**, 821–828 (2020).
[6] S. Kuwano, T. Suzuki, M. Yamanaka, R. Tsutsumi, and T. Arai, Angew. Chem. **131**, 10326–10330 (2019).
[7] M. G. Chudzinski, C. A. McClary, and M. S. Taylor, J. Am. Chem. Soc. **133**, 10559–10567 (2011).
[8] J. Y. C. Lim, I. Marques, A. L. Thompson, K. E. Christensen, V. Félix, and P. D. Beer, J. Am. Chem. Soc. **139**, 3122–3133 (2017).
[9] P. Molina, F. Zapata, and A. Caballero, Chem. Rev. **117**, 9907–9972 (2017).
[10] N. K. Shinada, A. G. de Brevern, and P. Schmidtke, J. Med. Chem. **62**, 9341–9356 (2019).
[11] F.-Y. Lin and A. D. MacKerell, Jr., J. Phys. Chem. B **121**, 6813–6821 (2017).
[12] Y. Lu, Y. Wang, Z. Xu, X. Yan, X. Luo, H. Jiang, and W. Zhu, J. Phys. Chem. B **113**, 12615–12621 (2009).
[13] L. Brammer, E. A. Bruton, and P. Sherwood, Cryst. Growth Des. **1**, 277–290 (2001).
[14] S. M. Malathy Sony and M. N. Ponnuswamy, Bull. Chem. Soc. Jpn. **79**, 1766–1772 (2006).
[15] J. Nadas, S. Vukovic, and B. P. Hay, Comput. Theor. Chem. **988**, 75–80 (2012).

[16]B. K. Saha, A. Saha, D. Sharada, and S. A. Rather, Cryst. Growth Des. **18**, 1–6 (2018).
[17]S. Dortéz, F. Fernández-Palacio, J. Damián, C. Gaiteiro, J. Ramos, P. Gómez-Sal, and M. E. G. Mosquera, CrystEngComm **22**, 870–877 (2020).
[18]W. Sattler, S. Ruccolo, and G. Parkin, J. Am. Chem. Soc. **135**, 18714–18717 (2013).
[19]W. A. Burns and K. R. Leopold, J. Am. Chem. Soc. **115**, 11622–11623 (1993).
[20]D. L. Fiacco and K. R. Leopold, J. Phys. Chem. A **107**, 2808–2814 (2003).
[21]D. L. Fiacco, Y. Mo, S. W. Hunt, M. E. Ott, A. Roberts, and K. R. Leopold, J. Phys. Chem. A **105**, 484–493 (2001).
[22]J. Grotewold, E. A. Lissi, and A. E. Villa, J. Chem. Soc. A **1966**, 1034–1037.
[23]J. Grotewold, E. A. Lissi, and A. E. Villa, J. Chem. Soc. A **1966**, 1038–1041.
[24]H. Kameo, Y. Baba, S. Sakaki, Y. Tanaka, and H. Matsuzaka, Inorg. Chem. **59**, 4282–4291 (2020).
[25]G. P. McGovern, D. Zhu, A. J. A. Aquino, D. Vidović, and M. Findlater, Inorg. Chem. **52**, 13865–13868 (2013).
[26]E. C. Escudero-Adán, A. Bauzá, C. Lecomte, A. Frontera, and P. Ballester, Phys. Chem. Chem. Phys. **20**, 24192–24200 (2018).
[27]S. J. Grabowski, ChemPhysChem **15**, 2985–2993 (2014).
[28]S. J. Grabowski, ChemPhysChem **16**, 1470–1479 (2015).
[29]Q. Tang and Q. Li, Mol. Phys. **113**, 3809–3814 (2015).
[30]M. X. Liu, H. Y. Zhuo, Q. Z. Li, W. Z. Li, and J. B. Cheng, J. Mol. Model. **22**, 10 (2016).
[31]Q.-Z. Li, L. Sun, X.-F. Liu, W.-Z. Li, J.-B. Cheng, and Y.-L. Zeng, ChemPhysChem **13**, 3997–4002 (2012).
[32]M. Michalczyk, W. Zierkiewicz, and S. Scheiner, ChemPhysChem **19**, 3122–3133 (2018).
[33]J. Zhang, Z. Wang, S. Liu, J. Cheng, W. Li, and Q. Li, Appl. Organomet. Chem. **33**, e4806 (2019).
[34]S. J. Grabowski, Phys. Chem. Chem. Phys. **19**, 29742–29759 (2017).
[35]S. Grabowski, Crystals **9**, 503 (2019).
[36]S. Grabowski, Molecules **20**, 11297–11316 (2015).
[37]S. J. Grabowski, Struct. Chem. **28**, 1163–1171 (2017).
[38]A. Bauzá and A. Frontera, Theor. Chem. Acc. **136**, 37 (2017).
[39]J. Zhang, Y. Wei, W. Li, J. Cheng, and Q. Li, Appl. Organomet. Chem. **32**, e4367 (2018).
[40]M. Jabłoński, J. Comput. Chem. **39**, 1177–1191 (2018).
[41]M. D. Esrafili and F. Mohammadian-Sabet, Struct. Chem. **27**, 1157–1164 (2016).
[42]Z. Chi, W. Dong, Q. Li, X. Yang, S. Scheiner, and S. Liu, Int. J. Quantum Chem. **119**, e25867 (2019).
[43]H. Ishikawa, A. Saito, M. Sugiyama, and N. Mikami, J. Chem. Phys. **123**, 224309 (2005).
[44]S. J. Grabowski, Coord. Chem. Rev. **407**, 213171 (2020).
[45]Z. Chi, Q. Li, and H. B. Li, Int. J. Quantum Chem. **120**, e26046 (2020).
[46]W. Dong, Y. Wang, X. Yang, J. Cheng, and Q. Li, J. Mol. Graphics Modell. **84**, 118–124 (2018).
[47]A. Bauzá and A. Frontera, ChemPhysChem **17**, 3181–3186 (2016).
[48]R. Berger, G. Resnati, P. Metrangolo, E. Weber, and J. Hulliger, Chem. Soc. Rev. **40**, 3496–3508 (2011).
[49]J. D. Dunitz and R. Taylor, Chem. Eur. J. **3**, 89–98 (1997).
[50]M. J. Frisch, G. W. Trucks, H. B. Schlegel *et al.*, Gaussian 09, Revision A.02, Gaussian, Inc., Wallingford, 2009.
[51]S. F. Boys and F. Bernardi, Mol. Phys. **19**, 553–566 (1970).
[52]F. A. Bulat, A. Toro-Labbé, T. Brinck, J. S. Murray, and P. Politzer, J. Mol. Model. **16**, 1679–1691 (2010).
[53]R. F. W. Bader, *AIM2000 Program, v.2.0* (McMaster University, Hamilton, Canada, 2000).
[54]A. E. Reed, L. A. Curtiss, and F. Weinhold, Chem. Rev. **88**, 899–926 (1988).
[55]P. Su and H. Li, J. Chem. Phys. **131**, 014102 (2009).
[56]M. W. Schmidt, K. K. Baldridge, J. A. Boatz, S. T. Elbert, M. S. Gordon, J. H. Jensen, S. Koseki, N. Matsunaga, K. A. Nguyen, S. Su, T. L. Windus, M. Dupuis, J. A. Montgomery, Jr., J. Comput. Chem. **14**, 1347–1363 (1993).
[57]S. Pan, A. Gupta, S. Mandal, D. Moreno, G. Merino, and P. K. Chattaraj, Phys. Chem. Chem. Phys. **17**, 972–982 (2015).
[58]S. J. Grabowski, J. Comput. Chem. **39**, 472–480 (2018).
[59]S. J. Grabowski, Molecules **25**, 2703 (2020).
[60]J. A. K. Howard, V. J. Hoy, D. O'Hagan, and G. T. Smith, Tetrahedron **52**, 12613–12622 (1996).
[61]M. S. Pavan, K. D. Prasad, and T. N. G. Row, Chem. Commun. **49**, 7558–7560 (2013).
[62]C. Dalvit, C. Invernizzi, and A. Vulpetti, Chem. Eur. J. **20**, 11058–11068 (2014).
[63]Z.-G. Hu, M. Yoshimura, K. Muramatsu, Y. Mori, and T. Sasaki, Jpn. J. Appl. Phys., Part 2 **41**, L1131–L1133 (2002).
[64]R. K. Li and Q. D. Zeng, J. Cryst. Growth **382**, 47–51 (2013).